



Cite this: *Anal. Methods*, 2019, **11**, 3648

## *In situ* silanization for continuous stationary phase gradients on particle packed LC columns

Anna V. Forzano, Caitlin N. Cain, Sarah C. Rutan \* and Maryanne M. Collinson \*

Mobile phase gradients are ubiquitous in liquid chromatography (LC); stationary phase gradients are not. Variation in the ligand density along the length of column can provide an important means to optimize separations. However, a major impediment relates to the development of methodologies to fabricate continuous gradient stationary phases, particularly on particle packed columns. For the first time, we demonstrate an *in situ* silanization approach based on the controlled rate infusion method to create a stationary phase gradient. This was accomplished by infusing a phenylbutyltrimethoxysilane solution through an in-house particle packed column for 1 h, with one end of the column being exposed longer than the other. Raman spectroscopy reveals a steep gradient over the first centimeter of the column followed by a plateau, indicating successful *in situ* modification. N<sub>2</sub> sorption experiments confirm the organosilane does not block the pores of the silica. The reversed phase (RP) and hydrophilic interaction liquid chromatography (HILIC) nature of the gradient stationary phase were evaluated using hydrophobic and hydrophilic probe analytes. The stability of the retention factors (RSD < 6%) and the column-to-column reproducibility (4% < RSD < 9%) were satisfactory. Surprising differences were observed in the amount of modification and the peak shapes for the gradient *versus* uniform stationary phases, which are partially attributed the nature of the on-column modification procedure. This work serves as a proof-of-concept for the constructive fabrication of continuous stationary phase gradients on particle packed columns and will hopefully stimulate future developments.

Received 7th May 2019

Accepted 21st June 2019

DOI: 10.1039/c9ay00960d

rsc.li/methods

## Introduction

Chemical gradients are ubiquitous in liquid chromatography (LC) when referring to mobile phase composition profiles; however, they are much less explored when referring to stationary phase ligand composition. The benefits of varying the ligand concentration along the length of column were first observed in the early 1990s with serially coupled columns<sup>1–6</sup> (*i.e.*, a discontinuous stationary phase gradient); however, the creation of a gradient on a *continuous* stationary support for LC did not come about until 2007, when Fanali *et al.* filled a capillary with solutions of decreasing hydrophilicities and used thermal polymerization to produce a stationary phase with a continuous hydrophobic gradient.<sup>7</sup> Since this work, the fabrication of continuous gradients in the stationary phase for LC has almost exclusively involved monoliths (polymer<sup>7–11</sup> and silica<sup>11,12</sup>), likely due to challenges associated with the formation of a gradient in chemical functionality on particle packed columns. To our knowledge, only one report has appeared on a continuous stationary phase gradient on a particle packed column.<sup>13</sup> In that work, the stationary phase gradient was

created on a commercially modified C<sub>18</sub> column *via* the time-dependent acid hydrolysis and hydrolytic cleavage of C<sub>18</sub> ligands.<sup>13</sup> For columns that have already been modified with an organic constituent, this is a viable approach for creating a stationary phase gradient on a packed column. However, there is still a need for the development of an *in situ* approach for the creation of a chemical gradient on a bare silica packed columns.

The interest in stationary phase gradients stems from a chromatographer's desire to improve selectivity and resolution, and provide possible peak focusing when a stationary phase gradient is coupled with a mobile phase gradient.<sup>13,14</sup> In contrast to discontinuous gradients, continuous gradients have the added benefit of novel selectivities that could arise from neighboring ligand effects, which can occur when two ligands are adjacent on a single chromatographic support.<sup>11,15</sup> Compared to traditional mixed-mode chromatography, which has a fixed ratio between the moieties along the length of the column,<sup>16</sup> the ligand ratio on a stationary phase gradient is not constant. Rather, the ligand ratio changes along the length of the column as dictated by the gradient shape or profile. As a result, the ligand ratio is not constant along the length of the column, and depending on the shape or profile of the gradient, unconventional selectivity could arise.<sup>11</sup> In order to further investigate this separation paradigm, methods for the

Chemistry Department, Virginia Commonwealth University, 1001 W Main St, Richmond, VA 23284-2006, USA. E-mail: [srutan@vcu.edu](mailto:srutan@vcu.edu); [mmcollinson@vcu.edu](mailto:mmcollinson@vcu.edu)



fabrication and detailed characterization of continuous stationary phase gradients are required.

In this work, we describe for the first time, an approach to fabricate and characterize a RP-HILIC stationary phase gradient on an in-house packed bare silica column using controlled rate infusion (CRI). This is a method developed by the Collinson group to form chemical gradients on planar substrates such as silicon wafers and thin layer chromatography plates using silane chemistry.<sup>17–21</sup> Our research on the use of this methodology to form a stationary phase gradient on a particle packed column *in situ* first began with the optimization of the type and the concentration of silane, along with the infusion parameters. The finalized method involved infusing a phenyl-butyltrimethoxysilane (PBTMOS) solution through a 5 cm long packed column containing particles that are 5  $\mu\text{m}$  in diameter ( $d_p$ ) to generate a phenyl–butyl gradient stationary phase. Uniform phenyl–butyl and uniform bare silica columns were also prepared as references. The columns were characterized with scanning electron microscopy (SEM), nitrogen ( $\text{N}_2$ ) sorption, Raman spectroscopy, and LC to fully evaluate this *in situ* fabrication method. The prime objective of this study was to develop a stable and reproducible method to form continuous stationary phase gradients to further research on their chromatographic behavior.

## Experimental

### Chemicals and reagents

Spherisorb bare silica particles ( $d_p = 5 \mu\text{m}$ , 80  $\text{\AA}$ , 220  $\text{m}^2 \text{g}^{-1}$ ) were purchased from Waters. PBTMOS (97%) and phenyltrimethoxysilane (PTMOS, 97%) were purchased from Alfa Aesar. Phosphoric acid (86%, ACS grade) and sodium acetate trihydrate crystal (99%) were purchased from J.T. Baker. Isopropanol (IPA, ACS grade), sodium phosphate monobasic (ACS grade), methanol (HPLC grade), toluene (ACS grade), hydrochloric acid (36.5–38% (w/w)), ammonium hydroxide (28–30% (w/w)), and benzoic acid (99.5%) were obtained from Fisher Scientific. Acetonitrile (ACN, UV grade) was purchased from Honeywell. Ethanol (200 proof, ACS grade) was purchased from Pharmco Aapers. Naphthalene (NAP, 99%), naphthol (NPOH, 98%), 2-aminopyridine (2-AP, 98%), chloroform (HPLC grade, 99.9%), uracil (98%), norepinephrine (NOR, 98%) and tyramine (TY) were purchased from Sigma Aldrich. Sodium hydroxide (97%, ACS grade) was purchased from Amresco. Nitrogen gas was purchased from Praxair. All water had a resistivity of 18.2  $\text{M}\Omega \text{ cm}$  and was obtained from a Milli Q system (Millipore Sigma, MA, USA).

### Column packing

All columns used in this report were packed in-house. Stainless steel ferrules, reducing unions and stainless-steel tubing (0.25"  $\times$  0.65" wall) were obtained from Swagelok. The assembled column casing (50  $\times$  4.6 mm) was attached to a Pack-in-a-Box dual head piston pump (Restek). The pushing solvent was 1 : 1 : 1 v/v toluene, ethanol, and IPA. The packing slurry was 7% w/v bare silica with 50 : 50 v/v methanol : chloroform. The slurry was sonicated for 3 to 5 minutes prior to pouring into the

packing chamber. Columns were packed for 1 h at 9000 psi and immediately detached from the column packer. A flat spatula was used to scrape any excess silica from the open end of the column, and the column was capped with a reducing union. More information can be found about packing columns in an article by Wahab *et al.*<sup>22</sup>

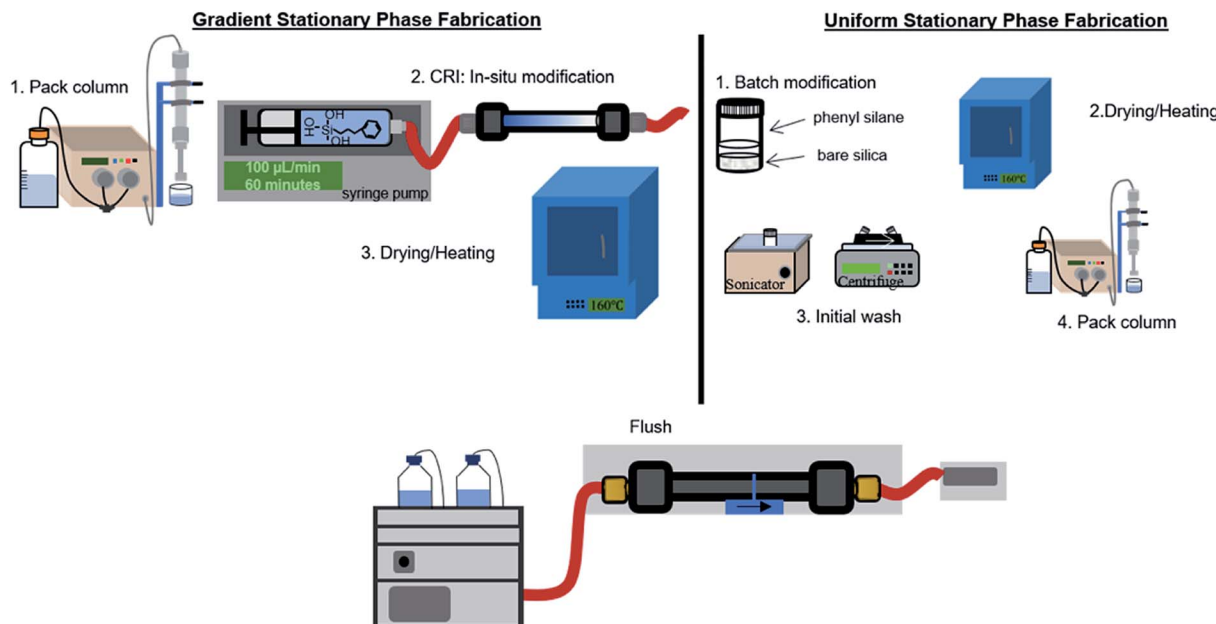
To verify the columns were chromatographically efficient before modification with CRI, the columns were attached to an LC (see Chromatographic characterization), injected with toluene and uracil (20  $\mu\text{g mL}^{-1}$  each), and the peak asymmetry factor ( $A_S$ , see Data analysis) for uracil evaluated using 90% ACN as the mobile phase. The average  $A_S$  for the columns used to create the phenyl butyl gradients was  $1.9 \pm 0.23$ . We recognize that the peak asymmetry of the columns prior to gradient modification is significantly higher than what would be expected for commercial columns. We choose to pack the columns in-house to ensure both the uniform and gradient columns were made from the same materials. Typically,  $A_S$  should be smaller than  $\sim 1.3$  to have a minimal effect on a separation.<sup>23</sup>

### Phenyl–butyl modification

Scheme 1 depicts the procedure used to form gradient (left) and uniform (right) phenyl–butyl columns. The PBTMOS solution was comprised of ethanol : PBTMOS : 0.1 M HCl : 0.2 M NaOH (906 : 140 : 200 : 80, v/v/v/v). To prepare the solution, ethanol, PBTMOS, and 0.1 M HCl were mixed for three hours and 45 minutes. NaOH (0.2 M) was added and the solution was stirred for another 15 minutes, totaling 4 h of stirring or 4 h of acid-catalyzed hydrolysis. Prior to modification to form the uniform phenyl–butyl material, bare silica was sonicated with ethanol for 30 minutes. Particles were centrifuged for 5 minutes at 2000g to remove ethanol. PBTMOS solution was added to a glass vial to prepare a 60% (v/w) PBTMOS solution : bare silica and the vial was placed on a rotisserie (LabQuake Vial Rotator, Barnstead Thermolyne) for 4 h. The particles were centrifuged for 5 minutes at 2000g to remove the PBTMOS solution and placed in a 40 °C oven overnight. The modified particles were heated at 160 °C for 1 h, allowed to cool and sonicated with ethanol for 15 minutes. The particles were centrifuged for 5 minutes at 2000g to remove ethanol and the particles were packed according to the procedure described earlier.

To prepare the gradient phenyl–butyl columns, a PBTMOS solution was prepared as described above. A bare silica column (50  $\times$  4.6 mm, 5  $\mu\text{m}$ , 80  $\text{\AA}$ ) was flushed at 1  $\text{mL min}^{-1}$  with ethanol for 60 column volumes ( $V_M$ ). A syringe pump (260D Syringe Pump with Controller, Teledyne) was used to infuse 6 mL of the PBTMOS solution at 100  $\mu\text{L min}^{-1}$  for 1 h over the bare silica column, exposing the entrance of the column to the hydrolyzed silane 6 minutes longer than the exit of the column. The column was back flushed with  $\text{N}_2$  (g) for 3 minutes at 100 PSI to encourage drying and then placed in a 40 °C oven overnight. The column was heated to 160 °C for 1 h, allowed to cool, and back flushed using an LC pump (1100 series, Agilent Technologies) with  $1000V_M$  ethanol : toluene (1 : 1, v/v),  $120V_M$  ACN,  $120V_M$  10 mM sodium acetate salt solution (pH 7.4  $\pm$  0.05),  $120V_M$  water, and  $120V_M$  ACN. This extensive washing





Scheme 1 Procedure for the fabrication of gradient and uniform phenyl–butyl particle packed columns for LC.

method is necessary to remove any excess reagent on the column. The use of sodium acetate minimizes any electrostatic interactions between hydrolyzed PBTMOS and the unreacted surface silanol groups.<sup>24,25</sup>

### Physical and chemical characterization

Once the columns were fully characterized chromatographically (see Chromatographic characterization) the silica was unpacked from the column for chemical and physical characterization with Raman spectroscopy, gas sorption, and SEM imaging.

Columns were flushed with  $10V_M$  of IPA prior to extrusion to fully wet the column bed. The entrance reducing union of the column was removed and the column was attached to an LC pump (1100 series, Agilent Technologies). The pump was set to flow IPA at  $0.2 \text{ mL min}^{-1}$ . The particles were pushed out slowly and 0.5 cm slices of the bed were obtained, totaling 10 slices from each column. The particles were dried overnight in a 40 °C oven prior to any analysis.

Samples containing 80–90% (w/v) particles : ethanol were prepared from each slice of the column (every 0.5 cm), which totals ten samples to evaluate the phenyl–butyl modification on the surface of silica. The solution was pipetted on to glass slides and dried briefly. The glass slides were placed on a Raman microscope using a 10× objective (LABRam HR Evolution Confocal Raman Spectrometer, Horiba) and three points ( $\sim 300 \mu\text{m}$  apart) were collected from each sample. The acquisition parameters were: 532 nm laser (50% power), spectral range from 900–3200  $\text{cm}^{-1}$ , 5 second acquisition time, with 24 accumulations, 600  $\text{g mm}^{-1}$  grating, 300  $\mu\text{m}$  slit and 1000  $\mu\text{m}$  pin hole. The laser spot size was  $\sim 2.6 \mu\text{m}$ .

Pore size distribution determination was performed by obtaining  $\text{N}_2$  adsorption and desorption isotherms of the uniform phenyl–butyl, uniform bare silica, gradient phenyl–

butyl columns (Quantachrome NOVA 2200e Surface Area and Pore Analyzer, Anton Parr). Samples of dried particles (0.35–0.6 g) were weighed out from positions: 0, 2.5, and 5 cm along each column. The samples were degassed at 100 °C for at least 12 h.

Barrett–Joyner–Halenda (BJH)<sup>26</sup> analysis was used to determine pore size distributions. The measurements were performed in duplicate and averaged.

SEM was used to investigate if the particle shapes or diameters were altered after gradient modification. A particle slurry (80–90% (w/v) particles : ethanol) was prepared using particles at the 0.5, 2.5 and 5 cm positions along each column. The solution was pipetted onto conductive carbon tape and dried. The particles were sputter coated with platinum for 90 seconds at 2.2 kV. Images were obtained with a SU-70 FE-SEM (Hitachi). Particle analysis was performed with ImageJ 1.52a software (National Institutes of Health), where 500 particles were measured<sup>22</sup> for bare silica samples and gradient samples (at the high phenyl–butyl region) to confirm that there was no change in particle diameter after modification.

### Chromatographic characterization

Chromatographic characterization of uniform phenyl–butyl, uniform bare silica, and gradient phenyl–butyl columns was performed for comparison purposes. The columns were attached to a LC-DAD (1260 Infinity, Agilent Technologies, CA, USA) and chromatographic runs were 1  $\mu\text{L}$  injections performed at  $1 \text{ mL min}^{-1}$ , with the column oven set to 40 °C. The DAD collected spectra from 190–400 nm, with a sampling interval of 2 nm. The mobile phase consisted of solvent A: 5 mM phosphate buffer (pH 2.5  $\pm$  0.05) and solvent B: ACN.

The stability of the uniform and gradient phenyl–butyl columns was evaluated through a sequence of 500 injections of NAP ( $20 \mu\text{g mL}^{-1}$ ) with 80 : 20 A : B as the mobile phase.



Isocratic characterization of uniform phenyl–butyl, uniform bare silica, and gradient phenyl–butyl columns was performed at 2, 10, 20, 30, 40, 50, 60, 70, and 80% B. Mixtures of benzoic acid, 2-aminopyridine, and naphthol (each 20  $\mu\text{g mL}^{-1}$ ) made in solvents matching the mobile phase compositions were used to probe the retention characteristics of the stationary phases. A mixture of naphthalene, naphthol, tyramine, norepinephrine, and 2-aminopyridine (each 20  $\mu\text{g mL}^{-1}$ ) were made up in 70% ACN, and injected on the uniform and gradient phenyl–butyl and uniform bare silica columns at 70% ACN to better understand the asymmetry factor.

### Data analysis

Chromatographic data were converted from Agilent \*.D files to MATLAB \*.mat files using ACD/Lab Spectrus Processor (Advanced Chemical Development, Inc., Toronto, Canada). MATLAB version R2017b (Mathworks, Inc, MA, USA) was used to resolve single analyte signals from the background and each other by performing multivariate curve resolution-alternating least squares (MCR-ALS) using an in-house built program.<sup>27</sup> An in-depth description of MCR-ALS can be found in the literature.<sup>28</sup> The pure chromatographic profile of each analyte produced from MCR-ALS was used to determine retention times and peak widths using statistical moment calculations,

$$M_0 = \sum_{i=1}^{\infty} h(t_i) \Delta t \quad (1)$$

$$M_1 = \frac{1}{M_0} \sum_{i=1}^{\infty} t_i h(t_i) \Delta t \quad (2)$$

$$M_2 = \frac{1}{M_0} \sum_{i=1}^{\infty} (t_i - M_1)^2 h(t_i) \Delta t \quad (3)$$

where  $h(t_i)$  is the height of the peak at time  $t_i$ , and  $M_0$ ,  $M_1$ , and  $M_2$  correspond to area, position ( $t_R$ ), and variance ( $\sigma^2$ ) respectively. Using eqn (2) to determine  $t_R$  is useful for peaks that show significant asymmetry, as opposed to simply using the maximum point of the peak. Retention factors ( $k$ ) were determined with the equation,  $k = (t_R - t_M)/t_M$  and asymmetry factor,  $A_S$ , was calculated using,  $A_S = B/A$ , where  $A$  is the distance from the front of the peak to the peak maximum and  $B$  is the distance from the peak maximum to the back of the peak at 10% of the peak maximum.<sup>29</sup>

Background noise from fluorescence of the silica powder was observed in the Raman spectra. To subtract the fluorescence background, the raw data were smoothed with Savitzky–Golay filter that produced a smoothed baseline that was subtracted from the raw data.<sup>30</sup> Numerical integration of the 999.4  $\text{cm}^{-1}$  band was then carried out on the background subtracted data.

## Results and discussion

### Fabrication of stationary phase gradient columns

Constructive CRI (*i.e.*, adding ligands to a substrate) is a cost-efficient and straightforward method to produce multicomponent chemical gradients on silica supports, by exposing one end

of a substrate longer than another to a hydrolyzed organosilane solution.<sup>17–21,31,32</sup> Adaption of constructive CRI to a particle packed column that is suitable for LC, however, has not been attainable until now. Compared to planar substrates and monolithic columns, the time-dependent modification of a traditional LC packed column *in situ* is much more challenging, not only because of the increased back pressure required for infusion into a packed column, but also because of the high surface area and microporosity of the silica powder. Additionally, porous particle columns have a lower permeability relative to monoliths,<sup>33</sup> which could potentially cause stagnant modification solution and unintentional heterogeneous modification.

The first step for gradient formation on a packed column involves optimization of the experimental parameters. In this work, the organoalkoxysilane (PTMOS vs. PBTMOS), the organoalkoxysilane solution (concentration (11 vs. 30% v/v), degree of hydrolysis (4, 12, 24 h)) and infusion parameters (infusion rate and volume (2 and 100  $\mu\text{L min}^{-1}$ ; 0.6 and 6 mL)) were specifically optimized, as these parameters strongly affect the degree of modification and hence the retention factors, peak shape, reproducibility, and long term stability. Using the retention factor ( $k$ ), % RSD of  $k$ , and peak shape for a nonpolar compound (naphthalene ( $k_{\text{NAP}}$ ) or naphthol ( $k_{\text{NPOH}}$ )) with a 20% ACN mobile phase composition ( $n = 3$  gradient columns) and a trial and error approach, the set of conditions that yielded columns with quantitatively reliable performances were found. The stationary phase gradients described herein were fabricated from a 6 mL PBTMOS sol (11% v/v) hydrolyzed for 4 h and infused at a flow rate of 100  $\text{mL min}^{-1}$  for 1 h, as these yielded the best results in terms of retention factor, peak shape, stability, and reproducibility.

### Characterization of phenyl–butyl gradient and uniformly modified stationary phases

The as-synthesized uniform and gradient modified columns were characterized using a number of different physical and chemical characterization tools. To ensure the organosilane did not over-polymerize and block the pores in the silica powder, which will result in poor mass transfer,  $\text{N}_2$  sorption experiments were undertaken. Fig. 1 shows the pore size distribution obtained from the packing material extruded from a uniform and gradient (at the high phenyl–butyl region, 0.5–1.0 cm) phenyl–butyl column. A comparison was also made to bare silica. As can be seen in Fig. 1, the pore size distributions are almost identical indicating the pores of the modified silica powder are not obstructed. Using BJH theory, the pore diameters were  $76.8 \pm 0.5$ ,  $77.2 \pm 0.4$ , and  $77.2 \pm 0.2 \text{ \AA}$  for each of the three columns (uniform bare silica, gradient phenyl–butyl, and uniform phenyl–butyl, respectively). The uniform (red) and gradient (blue) phenyl–butyl pore size distributions are slightly narrower than the uniform bare silica (yellow), likely due to the modification filling in some of the smaller pores.

In addition to porosity measurements, SEM was also used to inspect the particles after modification to determine if particle diameter significantly changed after CRI. Over modification,



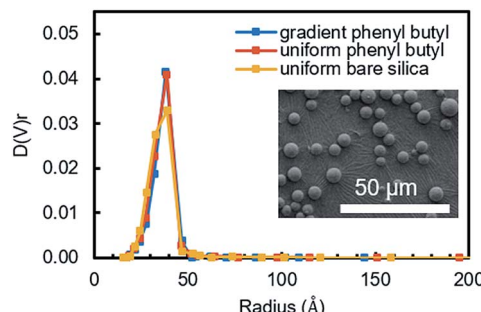


Fig. 1 Pore size distribution of silica powder extruded from the gradient phenyl–butyl at the high modified end (blue), uniform phenyl–butyl (red), and bare silica columns (yellow). Inset is a representative SEM of particles extruded from the highly modified end of the gradient column.

which would be evident by a change in diameter, would broaden chromatographic peaks and decrease the efficiency.

SEM images were obtained for particles at the entrance of a gradient column (high degree of modification, Fig. 1 inset) and for a bare silica sample for comparison. Using ImageJ, the diameter of 500 particles per sample ( $n = 3$  samples) were obtained and found to be equivalent to for bare silica ( $5.24 \pm 0.17$ ) and gradient particles ( $5.20 \pm 0.09$ ). Thus, it can be concluded that the chosen CRI parameters do not affect the diameter of the particles.

To chemically prove the existence of a stationary phase gradient, Raman spectroscopy was used on individual sections of the extruded column. The phenyl group shows a distinct stretching band near  $\sim 1000 \text{ cm}^{-1}$  due to strong in-phase ring stretching or breathing.<sup>34</sup> To complete the analysis, ten points (or samples) along the length of the column, each  $\sim 0.5 \text{ cm}$  apart were used to define the gradient profile. Three spots,  $\sim 300 \mu\text{m}$  apart, for each sample were irradiated with the  $532 \text{ nm}$  laser and averaged together to obtain spectra shown in Fig. 2B. Three Raman spectra for uniform bare silica, gradient phenyl–butyl, and uniform phenyl–butyl, respectively, are shown for comparison. The aromatic band can be clearly seen at  $999.4 \text{ cm}^{-1}$  on the modified silica (Fig. 2B and C), but not on bare silica (Fig. 2A), indicative of the presence of phenyl modification. Fig. 2B and C Raman spectra are from the entrance (0.5 cm, blue), middle (2.5 cm, red), and end (5.0 cm, yellow) of the gradient and uniform phenyl–butyl columns.

In Fig. 2C, for the uniform column, the three Raman spectra obtained from three different regions of the column are identical whereas in Fig. 2B, for the gradient column, the intensity is significantly larger at the entrance relative to the exit for all three columns. Quantitative assessment of the gradient profile was accomplished by measuring the area under the  $999.4 \text{ cm}^{-1}$  aromatic vibration. Fig. 2D shows the individual gradient profiles, where the area under the phenyl peak is plotted *versus* the distance along the column. A steep gradient can be noted along the first  $\sim 20\%$  of each of the three gradient columns. The phenyl–butyl modification associated with the first section of the gradient is significantly greater than the last section. Investigation of the total amount of phenyl–butyl deposited on each

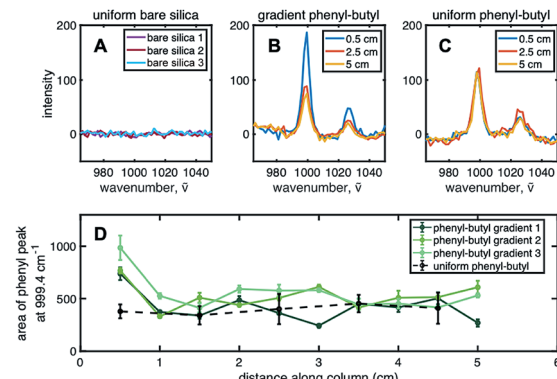


Fig. 2 Gradient profile characterization. Panel (A) is the Raman spectra collected from three bare silica samples (light blue, magenta, and maroon). Panels (B) (gradient phenyl–butyl) and (C) (uniform phenyl–butyl) are Raman spectra collected from the entrance (0.5 cm (blue)), middle (2.5 cm (red)), and exit (5 cm (yellow)) of the columns. Panel (D) is the area under the aromatic stretching band for phenyl–butyl gradient columns 1–3 (dark green, green, and light green lines, respectively), and uniform phenyl–butyl (dashed black line) as a function of distance along the length of the column. Error bars for gradient data represent three replicate Raman measurements on three different areas. Error bars for uniform phenyl–butyl data are from three uniform phenyl–butyl columns.

column was undertaken by summing the area of the  $999.4 \text{ cm}^{-1}$  peak for the three gradient columns, producing a % RSD of 15.2. This level of precision is deemed acceptable given the challenges associated with silane reactions because of their sensitivity to small variations in temperature, humidity, and silanol density.

Upon further examination of Fig. 2D, it can be seen that the area under the  $\sim 1000 \text{ cm}^{-1}$  band at the head of the gradient column is more than double that obtained on the uniform phenyl–butyl columns indicating that more phenyl groups are deposited on the surface of the particles during CRI *versus* *ex situ* batch modification. This is surprising given that the exposure time of the silica to the organosilane is  $4\times$  shorter during gradient formation. In other words, this represents an  $\sim 200\%$  increase in phenyl–butyl modification with an 75% reduction in reaction time.

### Chromatographic characterization

Different test mixtures were used to evaluate analyte retention, stability of modification, reproducibility between columns, and peak asymmetry ( $A_S$ ). The degree of modification of the stationary phase gradient columns was first evaluated by comparing chromatograms on uniform bare silica and phenyl–butyl columns to those on gradient phenyl–butyl columns (Fig. 3). The bare silica column produces a different elution order of 2-AP, benzoic acid and naphthol relative to the phenyl–butyl modified columns, indicating successful addition of phenyl–butyl to the silica. As expected, phenyl–butyl modified columns retain the relatively nonpolar probe analyte (naphthol) longer than the other more polar analytes, 2-AP and benzoic acid.

In the top panel of Fig. 4, the retention factors of naphthol *vs.* mobile phase composition are plotted, and as can be seen, naphthol is more retained on both modified columns relative to

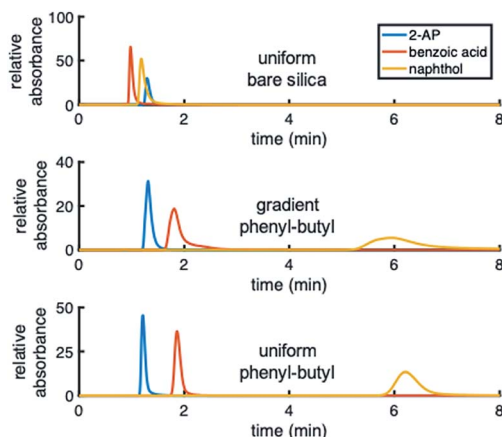


Fig. 3 Chromatograms obtained using bare silica (top), gradient phenyl–butyl (middle) and uniform phenyl–butyl (bottom) columns at 2% ACN. The uniformly modified phenyl–butyl has similar retention to the gradient phenyl–butyl.

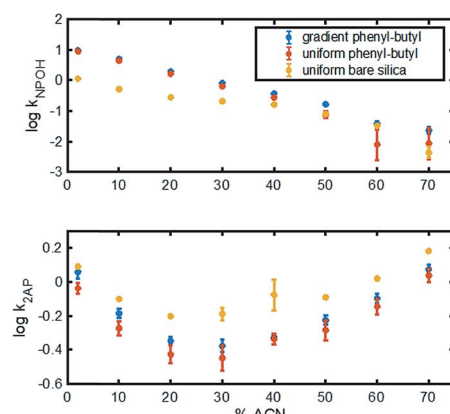


Fig. 4 Correlation between  $\log k$  and % ACN for naphthalene (top) and 2-AP (bottom) for phenyl–butyl gradient (blue), phenyl–butyl uniform (red), and bare silica uniform (yellow) columns. Error bars represent  $n = 3$  columns.

the bare silica column. Also noteworthy in Fig. 4 (top) is the approximate linear relationship between  $\log k$  vs. % ACN for the gradient and uniform phenyl–butyl columns. Such plots can assist in the elucidation of the separation mechanisms present.<sup>35</sup> The linear correlation between  $\log k_{\text{NPOH}}$  and % ACN with a negative slope in Fig. 4 (top) suggests RP behavior from the phenyl–butyl ligand. Fig. 4 (bottom) plots the relationship between the log of the retention factor of a more polar analyte, 2-AP, at various % ACN on uniform bare silica (yellow), gradient phenyl–butyl (blue) and uniform phenyl–butyl (red). A U-shaped plot can be noted for all three columns. The presence of a minimum, which in this case appears around 30–40% ACN, indicates there is a change in the separation mechanism. The dominant mechanism is no longer RP, but HILIC. Overall, the retention of the polar 2-AP is higher on the bare silica relative to the uniform and gradient phenyl–butyl, which is expected. The U-shape seen for both the uniform and gradient phenyl–butyl

columns, also indicates that both columns have silanol groups available for HILIC interactions. Endcapping of the uniform phenyl–butyl was purposely not performed to ensure that the uniform phenyl–butyl was a true positive control relative to the gradient.

The stability of the gradient columns was assessed with 500 injections<sup>36</sup> of uracil (dead time marker) and naphthalene (20  $\mu\text{g mL}^{-1}$  each) at 40% ACN. Fig. 5 shows overlaid chromatograms for the 50<sup>th</sup> and 500<sup>th</sup> injection at 40% ACN. The  $k_{\text{NAP}}$  value for the 500 injections was calculated using the first statistical moment from naphthalene and uracil peaks for each injection. The 500  $k_{\text{NAP}}$  values were plotted *versus* injection number to elucidate any trends. The retention factor drops by ~5% for the first 50 injections, and then begins to level off (Fig. 5 inset).

It was thus established that 50 equilibration injections (or  $166V_M$  of mobile phase) are needed before retention on the gradient stabilizes. Using injections #50 and #500, the %  $\text{RSD}_{\text{stability}}$  was calculated to be between 0.45 and 5.05% for  $n = 3$  columns. It can therefore be concluded that the gradient columns were stable, since the %  $\text{RSD}_{\text{stability}}$  for all three columns is under 7%, which is acceptable for the lifetime of a column.<sup>37</sup> Further investigation of stability was accomplished by calculating the %  $k_{\text{NAP}}$  loss for each column. The %  $k_{\text{NAP}}$  loss was found to be 0.51–6.8% ( $n = 3$  columns) for the gradient modified columns. The largest %  $k_{\text{NAP}}$  loss was under 7%.<sup>37</sup> Based on these results it can be concluded that this *in situ* modification method was successful for producing stable gradient columns.

The reproducibility of gradient column fabrication was also assessed chromatographically. Table 1 shows retention factors of a test mixture comprised of 2-AP, benzoic acid, and naphthalene. The  $\text{RSD}$  values for  $k_{2\text{-AP}}$ ,  $k_{\text{BA}}$ , and  $k_{\text{NPOH}}$  for the gradient columns are all under 10%, which confirms the suitability of these CRI conditions for reproducibly modifying columns for LC applications.

### Peak symmetry on gradient stationary phases

Upon examination of the chromatograms, it can be noted that the more hydrophobic analytes (e.g., naphthalene, naphthalene)

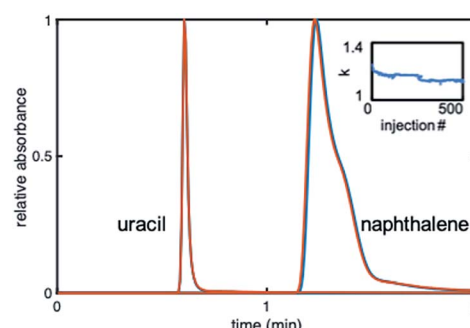


Fig. 5 Chromatograms depicting uracil and naphthalene at injections #50 (blue) and #500 (red) at 40% ACN on the gradient phenyl–butyl columns. Inset: The retention factor of naphthalene *versus* injection number.

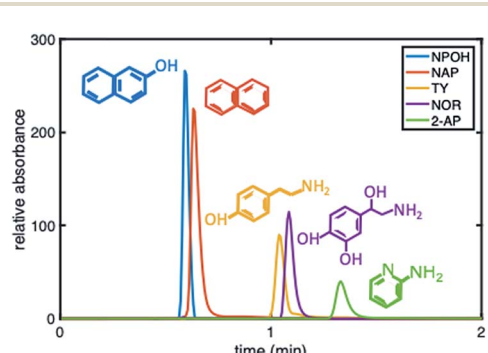
**Table 1** Comparison of retention factors at 20% ACN on three phenyl–butyl gradient columns

	2-AP	Benzoic acid	Naphthol
Gradient 1	0.47	0.63	2.13
Gradient 2	0.45	0.61	2.00
Gradient 3	0.43	0.54	1.77
% RSD	4.64	8.23	9.15

have peak shapes that are asymmetric, with  $A_S$  factors well above 2. For example, naphthalene in Fig. 5 has an  $A_S = 3.8 \pm 0.6$  ( $n = 3$  columns) at 40% ACN. For naphthol in Fig. 3 (middle),  $A_S = 4.4 \pm 1.3$  ( $n = 3$  columns) at 2% ACN. These analytes have significantly better peak shape on the uniformly phenyl–butyl modified column (e.g., Fig. 3 (bottom) with  $A_{S,NAP} = 2.12 \pm 0.14$  ( $n = 3$  columns)). Overloading was ruled out as a cause by decreasing the concentration of naphthalene from 20 to 10 and 5  $\mu\text{g mL}^{-1}$ . In spite of the lower concentrations, the tail of the peak remained.

Interestingly, the materials used to fabricate the uniform and gradient columns (e.g., bare silica and silane solution) are identical. Other than the spatial positions of the phenyl–butyl along the column, the only difference between the gradient and uniform columns relates to their method of modification. Gradients columns are made *in situ* via CRI, while the uniform columns are made *ex situ* in a batch mode (particles are modified first and then packed into the column). Before gradient modification, the particle packed silica columns have  $A_S = 1.9 \pm 0.2$  ( $n = 3$  columns) indicative that this observation is not related to the column packing.

To further demonstrate that the asymmetric peak shape is not the result of inefficient packing, a series of polar and nonpolar analytes (naphthol (NPOH), naphthalene (NAP), tyramine (TY), norepinephrine (NOR), and 2-AP) were injected on the gradient column and isocratically separated under a HILIC condition of 70% ACN, Fig. 6. From visual inspection of the chromatogram, it can be concluded that the peak shape of all the analytes (even retained ones) are significantly more symmetric ( $A_S \leq 2.2 \pm 0.4$  ( $n = 3$  columns)) relative to those

**Fig. 6** Chromatogram depicting the separation of five probe compounds of varying polarity with a 30 : 70 5 mM phosphate buffer, pH 2.5 : ACN on a phenyl–butyl gradient stationary phase.

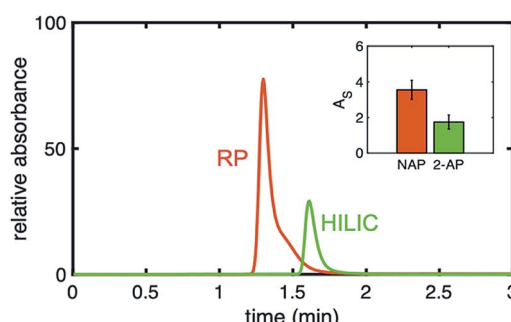
obtained under RP conditions, *e.g.*, 2% ACN (see Fig. 3 (middle)).

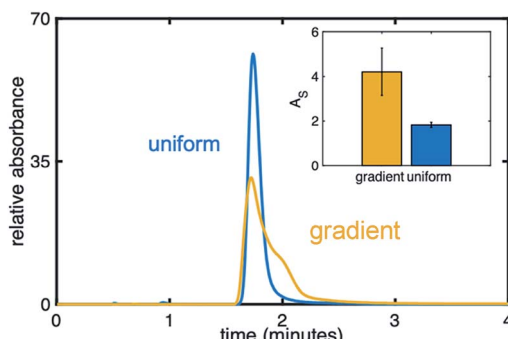
In Fig. 7, a direct comparison of the same gradient column using a nonpolar analyte, naphthol, under RP conditions and using a polar analyte, 2-AP under HILIC conditions is shown. Even though *it is the same column*, the injected analytes have very different peak symmetries ( $A_{S,NPOH} = 3.6 \pm 0.6$ ,  $A_{S,2-AP} = 2.2 \pm 0.4$ ), meaning when hydrophobic analytes interact with the phenyl–butyl gradients under RP conditions, unexpected peak shapes are produced. Again, this illustrates that column packing is not the cause of the asymmetric peaks.

Fig. 8 compares an injection of naphthol on a uniform (blue) and gradient (yellow) phenyl–butyl column at 20% ACN, a RP condition, while the inset depicts  $A_S$  values. The injection of naphthol on the gradient stationary phase gives rise to a significantly higher  $A_S$  relative to that observed on the uniform phenyl–butyl columns even though naphthol has a similar retention time on both columns. The appearance of an extra shoulder on the chromatographic peak obtained using the phenyl–butyl gradient column indicates a small fraction of the analyte is more strongly retained than the rest of the population, suggesting the possible presence of strong adsorption sites. Such sites, and thus the observed asymmetric peaks, are not seen on the uniform phenyl–butyl columns. We also don't believe that tailing is caused by free silanol groups, as nonpolar compounds, such as naphthalene, also show significant peak asymmetries.

One possible explanation for the peak asymmetry observed for the hydrophobic analytes on the gradient columns can be related to the distribution of phenyl groups on the surface of the silica particles due to differences in the way the silica particles are modified. *Ex situ* modification of the silica powder is expected to lead to a more even distribution of phenyl groups on the silica particles; on-column modification may produce phase separated domains<sup>38,39</sup> and thus the creation of strong adsorption sites.

For the uniformly modified column, the particles and phenyl–butyl silane are combined in a vial and placed on a rotisserie before being pressure-packed to create the column.

**Fig. 7** Chromatogram of naphthol (red, 30% ACN) and 2-AP (green, 70% ACN) acquired on the same phenyl–butyl gradient column but under two different mobile phase compositions. Inset: The asymmetry factors of naphthol at 30% ACN (red) and 2-AP at 70% ACN (green) on the same phenyl–butyl gradient. Column: Error bars represent  $n = 3$  columns.



**Fig. 8** Chromatogram of naphthol obtained on gradient (yellow) and uniform (blue) phenyl–butyl columns at 20% ACN. Inset: Asymmetry factors of naphthol on the gradient (yellow) and uniform (blue) phenyl–butyl columns.

For the gradient columns, modification is achieved *in situ* by flowing the silane through the packed bed followed by back flushing the residual silane out of the column with nitrogen. These important differences in exposure of the particles to the modifying silane may result in different orientations and densities of phenyl–butyl on the silica surface, particularly near the entrance. In fact, a higher density of phenyl groups is noted on the entrance of the gradient columns from the Raman experiments (Fig. 2D) as is the clustering of phenyl moieties near the entrance of the column. These peak broadening effects seen solely on the gradient columns demonstrate the interesting and complex behavior that chemical gradients can introduce, which warrants additional research. Future work includes creation of gradients with other ligands to investigate if this effect is unique to the phenyl–butyl ligand.

## Conclusion

Simulation<sup>14</sup> and experimental<sup>11,13</sup> data have demonstrated that continuous stationary phase gradients can offer novel selectivity and the potential for peak focusing. However, the fabrication of such gradients on particle packed columns is a major challenge and thus a significant obstacle to furthering research on continuous stationary phase gradient columns. Overcoming this hurdle involves the creation of a method to produce these columns *via in situ* modification. In this report, a time-based *in situ* method for the formation of a continuous phenyl–butyl multifunctional gradient stationary phase is described. The type of silane, infusion parameters, and modification/drying procedures were optimized to fabricate stable (% RSD < 6) and reproducible (% RSD < 10) continuous stationary phase gradients on particle packed columns. The gradient profile was confirmed with Raman spectroscopy. While the shapes of the chromatographic peaks indicate complex interactions, it is noteworthy that there are limited reports of *in situ* modification of particle LC columns, indicating that *in situ* modification is highly complex. Establishing a method of fabrication leads to the possibility to study the chromatographic behavior (*i.e.*, increased resolution and undiscovered selectivities) on these unprecedented stationary phases. This work represents the first

step towards realizing this goal. Continuation of this work will begin with increasing the chromatographic performance of this method, potentially using capillary columns, as well as modelling the dependence of the shape/slope of the gradient profile as a function of the synthetic experimental conditions.

## Conflicts of interest

The authors declare that there are no conflicts of interest.

## Acknowledgements

We gratefully acknowledge support for this work by the U.S. National Science Foundation Grant CHE-1609449. The authors also acknowledge the Nanomaterials Core Characterization Facility at Virginia Commonwealth University for use of the Raman microscope and SEM and Drs. Lena Jeong, Daniel Cook, and Joseph Turner for their helpful conversations and insights.

## References

- Y. Mao and P. W. Carr, Adjusting Selectivity in Liquid Chromatography by Use of the Thermally Tuned Tandem Column Concept, *Anal. Chem.*, 2000, **72**(1), 110–118.
- S. Nyiredy, Z. Szűcs and L. Szepesy, Stationary-Phase Optimized Selectivity LC (SOS-LC): Separation Examples and Practical Aspects, *Chromatographia*, 2006, **63**(S13), S3–S9.
- S. Nyiredy, Z. Szűcs and L. Szepesy, Stationary Phase Optimized Selectivity Liquid Chromatography: Basic Possibilities of Serially Connected Columns Using the “PRISMA” Principle, *J. Chromatogr. A*, 2007, **1157**(1–2), 122–130.
- T. Alvarez-Segura, C. Ortiz-Bolsico, J. R. Torres-Lapasió and M. C. García-Álvarez-Coque, Serial *versus* Parallel Columns Using Isocratic Elution: A Comparison of Multi-Column Approaches in Mono-Dimensional Liquid Chromatography, *J. Chromatogr. A*, 2015, **1390**, 95–102.
- J. Haggarty, M. Oppermann, M. J. Dalby, R. J. Burchmore, K. Cook, S. Weidt and K. E. V. Burgess, Serially Coupling Hydrophobic Interaction and Reversed-Phase Chromatography with Simultaneous Gradients Provides Greater Coverage of the Metabolome, *Metabolomics*, 2015, **11**(5), 1465–1470.
- T. Alvarez-Segura, J. R. Torres-Lapasió, C. Ortiz-Bolsico and M. C. García-Álvarez-Coque, Stationary Phase Modulation in Liquid Chromatography through the Serial Coupling of Columns: A Review, *Anal. Chim. Acta*, 2016, **923**, 1–23.
- A. Maruška, A. Rocco, O. Kornýšová and S. Fanali, Synthesis and Evaluation of Polymeric Continuous Bed (Monolithic) Reversed-Phase Gradient Stationary Phases for Capillary Liquid Chromatography and Capillary Electrochromatography, *J. Biochem. Biophys. Methods*, 2007, **70**(1), 47–55.
- S. Curran, D. Connolly, E. Gillespie and B. Paull, Fabrication and Characterisation of Capillary Polymeric Monoliths Incorporating Continuous Stationary Phase Gradients, *J. Sep. Sci.*, 2010, **33**(4–5), 484–492.



9 S. Curivan, D. Connolly and B. Paull, Production of Novel Polymer Monolithic Columns, with Stationary Phase Gradients, Using Cyclic Olefin Co-Polymer (COC) Optical Filters, *Analyst*, 2012, **137**(11), 2559.

10 S. Curivan, D. Connolly and B. Paull, Stepped Gradients on Polymeric Monolithic Columns by Photoinitiated Grafting, *J. Sep. Sci.*, 2015, **38**(21), 3795–3802.

11 V. C. Dewoolkar, L. N. Jeong, D. W. Cook, K. M. Ashraf, S. C. Rutan and M. M. Collinson, Amine Gradient Stationary Phases on In-House Built Monolithic Columns for Liquid Chromatography, *Anal. Chem.*, 2016, **88**(11), 5941–5949.

12 D. N. Bassanese, A. Soliven, X. A. Conlan, R. A. Shalliker, N. W. Barnett and P. G. Stevenson, A Non-Destructive Test to Assess the Axial Heterogeneity of *in situ* Modified Monoliths for HPLC, *Anal. Methods*, 2015, **7**(17), 7177–7185.

13 C. N. Cain, A. V. Forzano, S. C. Rutan and M. Collinson, Destructive Stationary Phase Gradients for Reversed-Phase/Hydrophilic Interaction Liquid Chromatography, *J. Chromatogr. A*, 2018, **1570**, 82–90.

14 L. N. Jeong and S. C. Rutan, Simulation of Elution Profiles in Liquid Chromatography – III. Stationary Phase Gradients, *J. Chromatogr. A*, 2018, **1564**, 128–136.

15 L. N. Jeong, R. Sajulga, S. G. Forte, D. R. Stoll and S. C. Rutan, Simulation of Elution Profiles in Liquid Chromatography – I: Gradient Elution Conditions, and with Mismatched Injection and Mobile Phase Solvents, *J. Chromatogr. A*, 2016, **1457**, 41–49.

16 L. Zhang, Q. Dai, X. Qiao, C. Yu, X. Qin and H. Yan, Mixed-Mode Chromatographic Stationary Phases: Recent Advancements and Its Applications for High-Performance Liquid Chromatography, *TrAC, Trends Anal. Chem.*, 2016, **82**, 143–163.

17 B. Kannan, D. Dong, D. A. Higgins and M. M. Collinson, Profile Control in Surface Amine Gradients Prepared by Controlled-Rate Infusion, *Langmuir*, 2011, **27**(5), 1867–1873.

18 B. Kannan, M. A. Marin, K. Shrestha, D. A. Higgins and M. M. Collinson, Continuous Stationary Phase Gradients for Planar Chromatographic Media, *J. Chromatogr. A*, 2011, **1218**(52), 9406–9413.

19 B. Kannan, D. A. Higgins and M. M. Collinson, Aminoalkoxysilane Reactivity in Surface Amine Gradients Prepared by Controlled-Rate Infusion, *Langmuir*, 2012, **28**(46), 16091–16098.

20 S. L. Stegall, K. M. Ashraf, J. R. Moye, D. A. Higgins and M. M. Collinson, Separation of Transition and Heavy Metals Using Stationary Phase Gradients and Thin Layer Chromatography, *J. Chromatogr. A*, 2016, **1446**, 141–148.

21 V. C. Dewoolkar, B. Kannan, K. M. Ashraf, D. A. Higgins and M. M. Collinson, Amine-Phenyl Multi-Component Gradient Stationary Phases, *J. Chromatogr. A*, 2015, **1410**, 190–199.

22 M. F. Wahab, D. C. Patel, R. M. Wimalasinghe and D. W. Armstrong, Fundamental and Practical Insights on the Packing of Modern High-Efficiency Analytical and Capillary Columns, *Anal. Chem.*, 2017, **89**(16), 8177–8191.

23 L. R. Synder, J. J. Kirkland and J. W. Dolan, *Introduction to Modern Liquid Chromatography*, John Wiley and Sons, Inc, 3rd edn, 2010, ch. 2.

24 J. Nawrocki, The Silanol Group and Its Role in Liquid Chromatography, *J. Chromatogr. A*, 1997, **779**(1–2), 29–71.

25 A. Méndez, E. Bosch, M. Rosés and U. D. Neue, Comparison of the Acidity of Residual Silanol Groups in Several Liquid Chromatography Columns, *J. Chromatogr. A*, 2003, **986**(1), 33–44.

26 E. P. Barrett, L. G. Joyner and P. P. Halenda, The Determination of Pore Volume and Area Distributions in Porous Substances. I. Computations from Nitrogen Isotherms, *J. Am. Chem. Soc.*, 1951, **73**(1), 373–380.

27 A. De Juan, J. Jaumot and R. Tauler, Multivariate Curve Resolution (MCR). Solving the Mixture Analysis Problem, *Anal. Methods*, 2014, **6**(14), 4964–4976.

28 S. C. Rutan, A. De Juan and R. Tauler, *Compr. Chemom.*, ed. S.D. Brown, R. Tauler and B. Walczak, Elsevier, 2009, vol. 2.

29 M. F. Wahab, D. C. Patel and D. W. Armstrong, Total Peak Shape Analysis: Detection and Quantitation of Concurrent Fronting, Tailing, and Their Effect on Asymmetry Measurements, *J. Chromatogr. A*, 2017, **1509**, 163–170.

30 M. U. A. Bromba and H. Ziegler, Application Hints for Savitzky–Golay Digital Smoothing Filters, *Anal. Chem.*, 1981, **53**(11), 1583–1586.

31 K. M. Ashraf, D. Giri, K. J. Wynne, D. A. Higgins and M. M. Collinson, Cooperative Effects in Aligned and Opposed Multicomponent Charge Gradients Containing Strongly Acidic, Weakly Acidic, and Basic Functional Groups, *Langmuir*, 2016, **32**(16), 3836–3847.

32 M. M. Collinson and D. A. Higgins, Organosilane Chemical Gradients: Progress, Properties, and Promise, *Langmuir*, 2017, **33**(48), 13719–13732.

33 T. Ikegami and N. Tanaka, Recent Progress in Monolithic Silica Columns for High-Speed and High-Selectivity Separations, *Annu. Rev. Anal. Chem.*, 2016, **9**(1), 317–342.

34 C. A. Doyle, T. J. Vickers, C. K. Mann and J. G. Dorsey, Characterization of Liquid Chromatographic Stationary Phases by Raman Spectroscopy Effect of Ligand Type, *J. Chromatogr. A*, 1997, **779**(1), 91–112.

35 J. G. Dorsey and W. T. Cooper, Retention Mechanisms of Bonded-Phase Liquid Chromatography, *Anal. Chem.*, 1994, **66**(17), 857A–867A.

36 C. Ye, G. Terfloth, Y. Li and A. Kord, A Systematic Stability Evaluation of Analytical RP-HPLC Columns, *J. Pharm. Biomed. Anal.*, 2009, **50**(3), 426–431.

37 S. J. Marin, B. A. Jones, W. D. Felix and J. Clark, Effect of High-Temperature on High-Performance Liquid Chromatography Column Stability and Performance under Temperature-Programmed Conditions, *J. Chromatogr. A*, 2004, **1030**(1–2), 255–262.

38 E. A. Smith and M. J. Wirth, pH Dependence of Tailing in Reversed-Phase Chromatography of a Cationic Dye: Measurement of the Strong Adsorption Site Surface Density, *J. Chromatogr. A*, 2004, **1060**(1–2 SPEC. ISS.), 127–134.

39 D. Giri, K. M. Ashraf, M. M. Collinson and D. A. Higgins, Single-Molecule Perspective on Mass Transport in Condensed Water Layers over Gradient Self-Assembled Monolayers, *J. Phys. Chem. C*, 2015, **119**(17), 9418–9428.

